Nov 16th, 12:00 AM

Behavior of C- and Z-purlins under Wind Uplift

Parviz Soroushian

Teoman Peköz

BEHAVIOR OF C- AND Z-PURLINS UNDER WIND UPLIFT

by

Teoman Peköz[1] and Parviz Soroushian[2]

INTRODUCTION

Cold-formed C- and Z-purlins are used widely in metal building roof systems. These sections are easy and economical to fabricate and erect. However they are weak in the lateral direction and in torsion. In order to use their full bending capacity in the strong direction, they must be braced in the lateral direction and against twisting. With proper attention to details, roof panels which are connected to the purlins do provide to some extent such bracing effect by virtue of their shear rigidity and resistance to local bending at the connections.

Wind uplift is an important design condition for roof purlins. The objective of the research reported herein was to develop simple design equations for C- and Z-purlins subject to uplift.

The previous work reported in Refs. 1, 6 and 7 based on the classical theory of torsional-flexure resulted in computer programs for the analysis of the problem. Due to its complexity the classical theory of torsional-flexure is not suitable for treating the effects of local buckling and post-buckling behavior on the overall behavior. Furthermore, this approach cannot be extended easily to include the effects of initial sweep and twist of purlins. The importance of these parameters was observed in several large scale tests. The theory was shown to be satisfactory for predicting deflections but not ultimate loads. The discrepancies were larger for thinner sections indicating the importance of local behavior of the component plate elements of the sections.

In the design of purlins the approach of Section of Part III of Ref. 6 is used quite frequently. This approach also has several deficiencies. First it is assumed that the compression flange of a purlin does not deflect laterally until failure. The actual behavior is clearly not so. The compression flange deflects laterally from the start of loading. Second, the effect of initial sweep and twist is not accounted for. These and several other additional deficiencies of that approach have been eliminated by the new approach derived in the research reported in this paper.

Large scale and component tests by the authors and by a metal building manufacturer have shown that the new approach is satisfactory for design purposes.

The research reported herein was conducted at Cornell University and sponsored by the American Iron and Steel Institute and the Metal Building Manufacturers Association. This paper is based primarily on Ref. 5. Early results of the research were reported in Ref. 8.

---

[1]Associate Professor of Structural Engineering, Cornell University, Ithaca, NY.

[2]Graduate Student, Cornell University, Ithaca, NY.

GENERAL THEORY

The previous work reported in Refs. 1, 6 and 7 has taken into account the bracing action of the roof panels due to their shear rigidity as well as the resistance to rotation by local bending at the purlin-to-roof-panel connection. The latter action will be referred to as the rotational restraint. The rotational restraint is also provided by the cross-bending rigidity of the panels. However, in the previous tests it was concluded that the cross-bending rigidity is an order of magnitude higher than the local rigidity at the connection. For this reason the rotations of the purlin due to cross-bending of the panels will be ignored.

In order to reach a simple solution and based on an intuitive assessment of the overall behavior in the building, the purlins will be assumed fixed against deflection in the plane of the roof at the purlin-to-roof-panel connection. This is equivalent to taking the value of the shear rigidity to be infinite in the method of analysis of Refs. 1, 6 and 7. This assumption appears reasonable on the basis of studies conducted using the computer program of Ref. 7. These studies show that as long as the value of the shear rigidity is larger than a reasonable minimum, this assumption is satisfactory for the simple solutions obtained in this research.

In a great majority of metal building applications, the purlins are continuous over the building frames which serve as intermediate supports for the purlins. The continuity is accomplished by lapping the purlins over the supports. The Z-purlins are lapped by nesting one inside the other. C-purlins are lapped by placing them back-to-back over the supports. In each case the purlins are bolted together and the screws connecting the roof panels to the purlins penetrate through both purlins. The research reported herein dealt with only simply-supported purlins. The solutions can be extended to continuous purlins as will be discussed below.

In this study as well as in the previous studies Refs. 1, 6 and 7, it is assumed that the load is in the initial plane of the web. It is assumed that load components perpendicular to the web will be supported by the roof panels. It is essential to provide proper means for anchoring these forces in the actual building. It is also assumed that through proper bracing the purlins are restrained against "rolling" (twisting and lateral bending) at the supports.

The C- and Z-purlins undergo vertical deflections and twisting. The twisting results in lateral deflections of the compression flange. Deflected configurations are shown in Fig. 1.a. For the purposes of our discussion and the derivation of the analytical model the deformations can be considered in two stages. These stages will be referred to as the torsion and the vertical bending stages. These stages are illustrated in Fig. 1.b.

The vertical bending stage can be analyzed using the simple flexure theory. However the moment of inertia is to be computed for the twisted section. Twisting does introduce some small vertical deflection component which will be added to the vertical deflections obtained for the vertical bending stage.

The torsion stage involves lateral deflection and twisting which will be analyzed through the use of an idealized analytical model. The model involves

the assumption of a beam-column on elastic foundation. The beam-column section consists of the compression flange and a portion of the web drawn with thick lines in Fig. 3. The spring constraint for the elastic foundation is obtained as follows. The purlin to panel connection can be idealized to act as a rotational spring located at the center of rotation of each purlin as shown in Fig. 2.a. Further simplification is made by converting this spring into a linear extensional spring of stiffness k located at the level of the compression flange shown in Fig. 2.a. This linear spring combines the effect of the restraint provided by the roof panels and the web of the purlin to the compression portion of the purlin. The roof panel restraint is best determined by test.

The lateral force on the idealized beam-column results from the variation of the shear flow along the member. In the case of Z-purlins, the center of rotation can be assumed to be the corner between the web and the tension flange and the flange shear flow force resultant causes a twisting moment about the center of rotation. The shear flow force in the web goes through the center of rotation and hence causes no twisting moment. On the other hand, the center of rotation for C-purlins can be assumed as the junction of the tension flange and its stiffener. In this case, the shear flow force in the web does not go through the center of rotation. Thus the shear force in the web, in addition to the shear force in the flange, causes a twisting moment about the center of rotation. The change in the shear force in the web per unit length is equal to the applied uniform vertical load q.

The distributed lateral load w(x) on the idealized beam-column (Fig. 2.b) results from the differences in the shear flow forces along the length of the member and can be expressed as

$$w(x) = \frac{\text{Flange Shear Force at } (x + dx) - \text{Flange Shear Force at } (x)}{dx} + \alpha q \tag{1}$$

$$w(x) = q\left(\frac{Qb}{2I} + \alpha\right) \tag{2}$$

where:

q = Distributed uplift load on purlin
b = Flange width (see Fig. 3)
Q = Static moment of the flange and the stiffening lip around the centroidal axis of the purlin
I = Moment of inertia about the horizontal axis of the section in the deflected configuration. Either the entire gross or the effective section is to be used as applicable. The determination of I will be discussed below and defined in Eq. 13
V = Shear force
H = Height of the section
α = The distance from the center of rotation to the junction of flange and web divided by the depth and 0 for Z-purlins

The first term of the right hand side of Eq. 1 represents the lateral loading on the idealized beam-column due to the shear flow in the compression flange and is the same for both the C- and the Z-purlin. For the sake of simplicity, the flange is assumed to be a flat element of width b (see Fig. 3).

This simplification is used only in determining w(x) and p(x) derived below. The second term of the same equation is to account for the twisting moment due to the shear force in the web. To facilitate the derivation below the loading in the web is converted to a load applied at the flange level and which results in the same twisting moment around the center of rotation as the load in the web.

The distributed axial force p(x) results from the variation of the compression stress along the length of the member. The beam-column section is assumed to be the flange and part of the flat width of the compression portion of the web BB($H/2 - R_1$) as shown in Fig. 3. The axial force can be expressed as follows:

$$p(x) = \frac{\text{Beam-Column Axial Force at } (x + dx) - \text{Beam-Column Axial Force at } (x)}{dx} \tag{3}$$

which is:

$$p(x) = V \cdot G \tag{4}$$

where

M = Bending moment at the section
G = Static moment of the beam-column area about the centroidal axis of the purlin divided by the moment of inertia
V = Shear force at any point in the span (function of x) = dM/dx

With the above idealizations the analysis of C- and Z-purlins for lateral deflections and twisting (torsion stage) is reduced to the analysis of the beam-column section shown in Fig. 3 with the loading shown in Fig. 2.b.

The strain energy consists of two parts: the flexural strain energy (U_f), and the elastic foundation strain energy (U_k). Their values are:

$$U_f = 2 \int_o^{\ell/2} \frac{EI_f}{2} \left(\frac{d^2u}{dx^2} - \frac{d^2u_o}{dx^2}\right)^2 dx \tag{5}$$

$$U_k = 2 \int_o^{\ell/2} \frac{K(u - u_o)^2}{2} dx \tag{6}$$

where

I_f = Moment of inertia of the beam-column around its own centroidal axis parallel to the web
L = Span of the beam-column
K = Stiffness of the linear spring
u = Deflection of the beam-column in the plane of the flange
u_o = Initial sweep of the beam-column in the plane of the flange
E = Modulus of elasticity

The potential energy of the external loads also has two parts: that of the lateral loads (U_w), and the axial loads (U_p). Their values are:

$$U_w = -2 \int_o^{\ell/2} w(x) \cdot (u - u_o)\, dx \tag{7a}$$

$$U_p = -2 \int_o^{\ell/2} \left\{ p(x) \cdot \frac{1}{2} \int_x^{\ell/2} \left[\left(\frac{du}{dx}\right)^2 - \left(\frac{du_o}{dx}\right)^2 \right] dx \right\} dx \tag{7b}$$

The total potential energy can be expressed as

$$U = V_f + V_k + W_w + W_p \tag{8}$$

SOLUTION

In this section the total potential energy equations derived above will be solved by the Ritz procedure. The procedure involves the use of trigonometric functions satisfying the end conditions as well as the conditions at intermediate braces where applicable. Solutions for various intermediate bracing conditions are given in Ref. 1. In this paper only the solution for the case of no intermediate bracing will be covered.

The following displacement functions satisfy the end conditions for the simply supported purlins:

$$u = \sum_{n=1,3,\ldots}' a_n \cdot \sin \frac{n\pi x}{\ell} \tag{9}$$

$$u_o = \sum_{n=1,3,\ldots}' a_{no} \sin \frac{n\pi x}{\ell} \tag{10}$$

where a_n are the amplitude of deflections to be computed using the energy expressions and a_{no} are the amplitudes which can be obtained from the measured values of the sweep in the plane of the flange. Since the lateral deflections are symmetric with respect to the midspan, only the odd values of n are used in the solution.

The amplitudes a_n can be determined by the Ritz procedure as:

$$a_n = \frac{4q\ell^4\left(\frac{Qb}{2I} + \alpha\right) + a_{no}\left(n^5 EI_f \pi^5 + nK\ell^4\pi\right)}{EI_f\pi^5 n^5 + K\ell^4 n\pi - 4Gq\ell^4 n\pi(.206n^2 - .063)} \tag{11}$$

It should be noted that the lateral deflection, u, is the total lateral deflection of the compression flange including the initial sweep. The deflections of the vertical bending stage does not have a component in the plane of the flange. However the lateral deflection, u, causes a deflection component in the vertical direction. The vertical deflection component is shown in Fig. 4. The total vertical deflection, v, can be expressed as follows:

$$v = \frac{qx}{24EI}\left(\ell^3 - 2\ell x^2 + x^3\right) + \frac{\psi u^2}{2H} \tag{12}$$

where ψ is a correction factor which will be discussed in the next section.

As a result of lateral deflections and twist, the moment of inertia with respect to the centroidal axis perpendicular to the original position of the web will be reduced. The following simple approximate expression for the reduced moment of inertia is obtained in Ref. 5:

$$I = I_o\left[1 - \left(\frac{u}{H}\right)^2\right] \tag{13}$$

where I_o is the moment of inertia of the total or effective section about the centroidal axis perpendicular to the web.

The total stresses in the purlin are obtained by superposing the stresses due to bending in the plane of the web (the vertical bending stage) on the stresses due to twisting and lateral deflection (torsion stage). Thus the total stress can be expressed as

$$\sigma = \frac{M}{S} + \frac{M_f}{S_f} \tag{14}$$

where

M = Moment resulting from the vertical bending stage = $q(l - x)/2$
S = Section modulus based on the moment of inertia I
S_f = Section modulus of the beam-column about its centroidal axis parallel to the web
M_f = Beam-column bending moment

The beam-column bending moment M_f can be determined as follows:

$$M_f = EI_f\left(u'' - u_o''\right) \tag{15}$$

$$M_f = \frac{EI_f\pi^2}{\ell^2} \cdot \sum_{n=1,3,\ldots} n^2\left(a_n - a_{no}\right) \sin\frac{n\pi x}{\ell} \tag{16}$$

The maximum compressive stress occurs at the junction of the compression flange with the web. Thus, S_f to be used in Eq. 12 should be the appropriate section modulus for that point.

Numeric studies were conducted using practical values of the parameters involved. These studies have shown that the series used in the Ritz procedure solution converges rapidly. Taking only one term of the series leads to errors in u less than 5 percent. For n = 1, a_n becomes

$$a_1 = \frac{C_1\left(\frac{Qb}{2I} + \alpha\right) + a_{1o}}{1 - .45C_1G} \tag{17}$$

where

$$C_1 = \frac{1.27q}{\frac{94.41EI_f}{\ell^4} + K} \tag{18}$$

The flange bending moment can now be found using Eq. 16. Due to the term n^2 in the summation, taking only the term with n = 1 leads to less accurate results. Namely, the convergence is less rapid for the flange bending moment than that for the lateral deflection. However, with proper simplifications, as will be described below, taking n = 1 even for the flange bending moment gives excellent results.

Parametric studies and the evaluation of the test results lead to the following simple approach. If the portion of the web contributing to I_f, Q, and G is ignored and the compression flange width is taken to be equal to b as shown in Fig. 3 then

$$I_f = tb^3/12 \tag{19}$$

$$G = btH/(4I_o) \tag{20}$$

and

$$Q = btH/2 \tag{21}$$

Substituting Eqs. 19 through 21 into Eqs. 17 and 18, the following is obtained

$$a = \frac{C(Zb + \alpha) + a_o}{1 - .9ZC} \tag{22}$$

where

$$Z = \frac{tHb}{4I_o} \tag{23}$$

$$C = \frac{1.27q}{\frac{7.87Etb^3}{\ell^4} + K} \tag{24}$$

α was defined in connection with Eq. 2. All parameters should have consistent units.

In the above equations the notation has been simplified by expression C_1 as C, a_1 as a, and a_{1o} as a_o. Furthermore, for simplicity, the reduction in the moment of inertia is ignored. Using Eq. 14 and the simplifications discussed above, the expression for the maximum stress at the flange to web junction for Z-purlins and flange to stiffening lip junction of C-purlins becomes

$$\sigma = \frac{MH}{2I} + \frac{Eb\pi^2}{2\ell^2}(a - a_o) \tag{25}$$

M is defined in connection with Eq. 14, I is defined by Eq. 13 with u = the amount of lateral deflection for lateral load q. The following procedure for determining the value of K in the above equations gave good results. The horizontal force, w(x), at which the value of K is determined can be found by Eq. 2. With the simplifications above this equation becomes

$$w = q\left(\frac{b^2 tH}{4I_o} + \alpha\right) \tag{26}$$

Units of w are in lbs/in.

The solution involves a very rapidly converging iteration. In this iteration, first a failure load q is assumed. Then the value of w is determined. From a plot of lateral load versus lateral displacement of an F test (described below), the value of K is determined at a load equal to w.

The total maximum vertical deflection can be obtained from Eq. 12 by setting $x = \ell/2$

$$v_{max} = \frac{5q\ell^3}{384EI} + \frac{\psi a^2}{2H} \tag{27}$$

The first term in the above equation is the component due to vertical bending. $a^2/(2H)$ in the second term is due to lateral bending as shown in Fig. 4. The factor ψ is to account for the cross-sectional distortion effects. It should depend on the cross-sectional dimensions. However, a regression analysis (Ref. 5) conducted on the test results indicated that taking a value of 3.4 for ψ leads to good agreement between the computed and observed results.

FAILURE CRITERIA

Under uplift loading simply supported purlins deflect as shown in Fig. 1.a. Thus, in general the maximum compressive stress occurs at the junction of the web-to-compression flange. With only a few exceptions, the dominant failure mechanism observed in the large scale tests was the formation of an inelastic local buckle at the web to compression flange junction. For this reason various procedures of predicting web failure were used in the research to formulate a purlin failure criterion. However, here only the procedure adopted in the 1980 AISI Specification (Ref. 9) will be discussed. In this approach based on Ref. 4 a failure stress is defined. The web is taken as fully effective. In the application of this approach, the beam-column section was assumed to be the compression portion of the section with BB (see Fig. 3) taken equal to zero.

If the compression flange is a stiffened plate element, the failure stress, F_{wu}, taken as

$$F_{wu} = \left[1.210 - .000337\left(\frac{H}{t}\right) \cdot \sqrt{F_y}\right] \cdot F_y \leq F_y \tag{28}$$

where F_y is the yield stress of the material.

If the compression flange is an unstiffened plate element the F_{wu} becomes

$$F_{wu} = \left[1.259 - .000508\left(\frac{H}{t}\right) \cdot \sqrt{F_y}\right] \cdot F_y \leq F_y \tag{29}$$

For the Z-purlins with inclined stiffeners, the web failure stress equation for unstiffened flanges was used in all cases.

For the C-purlins the decision whether the flange is stiffened or not was based not on the AISI Specification but on the procedure proposed in Ref. 3 as follows:

$$\text{Define } R = \frac{w}{t}\ ,\ R_\alpha = \frac{221}{\sqrt{F_y}}\ ,\ R_\beta = \frac{77.23}{\sqrt{F_y}} \tag{30}$$

where

w = Flat width of flange
t = Thickness

$$\text{If } R \leq R_\beta : I_{s_{adeq.}} = 0 \tag{31}$$

$$\text{If } R_\beta \leq F \leq R_\alpha : I_{s_{adeq.}} = 389t^4\left(\frac{R}{R_\alpha} - .324\right)^3 \tag{32}$$

$$\text{If } R \geq R_\alpha : I_{s_{adeq.}} = t^4\left(\frac{115R}{R_\alpha} + 5\right) \tag{33}$$

If I_s is $< I_{s_{adeq.}}$, assume the flange to be unstiffened.

If $I_s \leq I_{s_{adeq.}}$, assume the flange to be stiffened.

As mentioned above, the dominant mode of failure in the tests was due to yielding or local buckling at the flange to web junction. In a roof system, under certain circumstances, web crippling may occur. Therefore, this type of failure also needs to be checked separately.

The compression flanges in all the tests were fully effective according to the findings of Ref. 3. If the compression flange is not fully effective the simple design approach above needs to be modified by taking the effective portions of the flange in Eqs. 19 through 24.

Further complications may arise if the initial purlin imperfection is such that maximum stress may occur at the flange tip. In this case the criteria of Ref. 3 would probably have to be modified. Further studies on this subject are being conducted at the present time.

EXPERIMENTS

A rather extensive testing program was undertaken to check the validity of the several assumptions and simplifications made in the development of the analytical model.

An overview of the previous tests conducted under the supervision of the senior author is given in Ref. 6. In the present study, further variation of the cross-sectional dimensions was sought. Thus, basically two types of experiments were conducted: large scale purlin roof panel assembly tests and small scale component tests.

All large scale tests were conducted on 20 foot span simply-supported purlins. In the first phase of the research reported in Ref. 8, seven two-purlin assemblies were tested under four point loading. Subsequently, all tests were conducted on purlin roof panel assemblies subjected to vacuum loading. The details of test set-up and procedure are reported in Refs. 5 and 8.

In addition to the tests conducted at Cornell University, a series of tests were conducted by a metal building manufacturer. The results of these tests, some of which were observed by the senior author, were made available for evaluation by the researchers. The dimensions of the purlins used in the vacuum tests are listed in Table 1. The vacuum test results are presented in Table 2.

Component tests consisted of materials properties tests, diaphragm shear rigidity (cantilever shear) tests and rotational restraint (F) tests. These tests are again described in detail in Refs. 5 and 8. The rotational restraint test was used to determine the spring constant K used in the analysis. Fig. 5 illustrates the set-up for rotational restraint test. This test set-up was suggested by R. W. Haussler.

CORRELATION OF OBSERVED AND CALCULATED RESULTS

Table 2 summarizes the results of the vacuum tests. In this table the test results are compared with the calculated results. The ultimate load calculated using the simplified equations 19 through 25 is designated q_{os} in this table. The ultimate load calculated using equations 11 through 16 by taking n = 1 is designated by q_o. It is seen that the correlation is satisfactory. The use of other failure criteria and the convergence of the series solutions are explored in Ref. 5.

GRAVITY LOADING

Work is presently underway to extend the ideas developed and used in this research to the case of gravity loading. In the case of gravity loading, taking proper account of the roof shear rigidity and the behavior of stiffening lips is essential. The latter point is due to the fact that under gravity loading the lateral bending stress adds to the vertical bending stress at the stiffening lip. In the case of uplift loading, the lateral bending stress reduces the total stress at the stiffening lip.

SUMMARY AND CONCLUSIONS

The behavior of C- and Z-purlins braced by roof panels was studied for wind uplift loading. The analytical formulation of the behavior included several important parameters that have not been considered previously.

A very simple approach was developed to predict behavior. This approach correlated well with the results of a rather extensive experimental program.

The research dealt primarily with simply supported purlins. However, the results can readily be extended to multiple span continuous purlins by considering the portions between the inflection points as simply supported.

Though not presented here, some solutions for the intermediately braced purlins were also developed. Work is currently underway at Cornell University to apply the ideas developed in this research to the case of gravity loading in order to formulate simple design provisions.

The design procedure for wind uplift loading is being considered for inclusion in the AISI Specification by a task group of the AISI Specification Advisory Committee.

Appendix.--References

1. Celebi, N., Peköz, T. and Winter, G., "Behavior of Channel and Z-Section Beams Braced by Diaphragms," Proc. of First Specialty Conference on Cold-Formed Steel Structures, University of Missouri-Rolla, 1971.

2. "Cold-Formed Steel Design Manual," American Iron and Steel Institute, Washington, D.C., 1977 edition.

3. Desmond, T.P., Peköz, T. and Winter, G., "Edge Stiffeners for Thin-Walled Members," Journal of the Structural Division, ASCE, Vol. 107, No. ST2, Proc. Paper 16056, February 1981, pp. 329-351.

4. LaBoube, R.A. and Yu, W-W., "Webs for Cold Formed Steel Flexural Members," Civil Engineering Study 78-1, Structural Series, University of Missouri-Rolla, Final Report June 1978.

5. Peköz, T. and Soroushian, P., "Behavior of C- and Z-Purlins under Wind Uplift," Dept. of Structural Engineering Report, No. 81-2, Cornell University, February 1982.

6. Peköz, T., "Progress Report on Cold-Formed Steel Purlin Design," Proceedings of the Third International Conference on Cold-Formed Steel Structures, Dept. of Civil Engineering, University of Missouri-Rolla, November 1975.

7. Peköz, T., "Diaphragm Braced Channel and Z-Section Purlins," Report and Computer Program prepared for MBMA and AISI, 1973.

8. Razak, M.A.A. and Peköz, T., "Progress Report - Ultimate Strength of Cold-Formed Steel Z-Purlins," Dept. of Structural Engineering Report No. 80-3, Cornell University, February 1980.

9. "Specification for the Design of Cold-Formed Steel Structural Members," American Iron and Steel Institute, Washington, D.C., September 3, 1980 edition.

Appendix.--Notation

a_n	Amplitude of the lateral deflection of the beam-column ($a_1 = a$)
a_{no}	Amplitude of the initial sweep of the beam-column ($a_{1_o} = a_o$)
BB	Portion of the compression segment of the web included in the beam-column analysis
b	Total flange width (Fig. 3)
E	Modulus of elasticity
F_{wu}	The failure stress at the junction of the compression flange to web
F_y	Yield stress
G	Static moment of the beam-column area about the centroidal axis of the purlin divided by the moment of inertia of the section
H	Total height of the section
I	Moment of inertia about the horizontal axis (normal to the undeflected web) for the section in the deflected configuration
I_o	Moment of inertia about the horizontal axis (normal to the undeflected web) for the section in the undeflected configuration
I_f	Moment of inertia of the beam-column around its centroidal axis parallel to the web
I_s	Moment of inertia of the flange stiffener around its own centroidal axis
K	Stiffness of the spring located at the level of the compression flange
M_f	Bending moment in the beam-column
M	Bending moment in the purlin resulting from the vertical bending stage
p(x)	Distributed axial force on the beam-column at distance x from the support
Q	Static moment of the flange and the stiffening lip around the centroidal axis of the purlin
q	Distributed wind vacuum load on the C- or Z-purlin
R_1	Radius of curvature of the junction between the compression flange and the web
S	Section modulus of the purlin

S_f Section modulus of the beam-column around its own centroidal axis parallel to the web, for calculating stresses at the junction of the compression flange to the web

t Thickness of the section

U Total potential energy of the beam-column

U_f Flexural strain energy of the beam-column

U_k The elastic foundation strain energy of the beam-column

U_p The potential energy of the axial loads on the beam-column

U_w The potential energy of the lateral loads on the beam-column

u Total deflection of the beam-column in the plane of the compression flange

u_o Initial sweep of the beam-column in the plane of the compression flange

V Shear force in the purlin

v Total vertical deflection of the web to compression flange junction

w Flat width of the compression flange

$w(x)$ Distributed lateral load on the beam-column

x Distance along the length of the purlin from the simple support

α The value of b/H for C-purlins and zero for Z-purlins

ℓ Span of the simply supported purlin

ψ Correction factor to account for the cross-sectional distortion effects on the calculation of the vertical component of deflection from torsion (Fig. 4)

σ The maximum stress at the junction of the web to compression flange

TABLE 1

CROSS-SECTIONAL DIMENSIONS**

Section ($H \times t \times a_o$)	H (in)	t (in)	w (in)	α (rad)	R (in)	R_1 (in)	S (in)	F_y (ksi)
Z 8 x .059 x .1	8	.059	1.961	.624	.49	.578	.624	66.00
Z 7.92 x .06 x .56*	7.92	.060	2.01	.698	.392	.300	.640	61.50
Z 8.055 x .063 x .25	8.055	.063	2.059	.873	.477	.279	.602	56.89
Z 7.97 x .07 x .25	7.97	.070	1.875	.698	.715	.527	.766	64.60
Z 8 x .075 x .25	8.00	.075	1.891	.716	.738	.551	.734	64.70
Z 8.031 x .088 x .25	8.031	.088	1.953	.707	.762	.461	.727	63.80
Z 8 x .089 x .00	8.00	.089	1.938	.751	.688	.498	.797	64.00
Z 7.94 x .114 x .25	7.94	.114	2.051	.831	.746	.309	.773	56.1
Z 7.93 x .115 x .47*	7.93	.115	1.860	.620	.805	.445	.810	65.90
Z 9.625 x .062 x .125	9.625	.062	2.141	.799	.656	.402	.875	57.44
Z 9.45 x .063 x .66*	9.45	.063	2.030	.733	.512	.326	.600	57.3
Z 9.578 x .106 x -.0625	9.578	.106	2.141	.712	.523	.367	.602	52.90
Z 9.49 x .109 x .25*	9.49	.109	2.020	.698	.680	.34	.900	57.60
C 7 x .075 x .00*	7.00	.075	1.656	1.571	.406	.406	.359	55.0
C 9 x .075 x .25*	9.00	.075	1.750	1.571	.320	.306	.445	55.25
C 9 x .077 x 1.0*	9.00	.077	1.820	1.571	.328	.318	.420	55.25

*All sections marked by an asterisk were tested at Cornell University. All others were tested by a metal building manufacturer.

**Cross-sectional notation is illustrated in Fig. 3.
α is the angle of the stiffening lip with the horizontal (flange).

TABLE 2

COMPARISON OF OBSERVED AND CALCULATED ULTIMATE LOADS*

Section (H x t x a_o)	q_{test}	q_{cs}	q_c	$\frac{q_{cs}}{q_{test}}$	$\frac{q_c}{q_{test}}$
Z 8 x .059 x .1	90.7	102	109.2	1.12	1.20
Z 7.92 x .06 x .56**	83	98.4	102.0	1.19	1.23**
Z 8.053 x .063 x .25	96.2	105.6	108	1.10	1.12
Z 7.97 x .07 x .25	118.35	128.4	138.0	1.08	1.17
Z 8 x .075 x .25	137.9	136.8	146.4	0.99	1.06
Z 8.031 x .088 x .25	165.8	168.0	176.4	1.01	1.06
Z 8 x .089 x .00	162.7	174.0	181.2	1.05	1.09
Z 7.94 x .114 x .25	214.5	210.0	213.6	0.98	1.00
Z 7.93 x .115 x .47	184.0	218.4	229.2	1.19	1.25
Z 9.625 x .062 x .125	119.0	103.2	104.4	0.87	0.88
Z 9.45 x .063 x .66	114.0	102.0	103.2	0.89	0.91
Z 9.578 x .106 x -.0625	266.7	218.4	220.8	0.82	0.83
Z 9.49 x .109 x .25**	218.0	201.6	205.2	0.92	0.94**
C 7 x .075 x .00	127.3	102.0	116.4	0.80	0.91
C 9 x .075 x .25	117.2	102.0	109.2	0.87	0.93
C 9 x .077 x 1.0	103.2	94.8	103.2	0.92	1.00
Mean				0.99	1.04
Coefficient of variation (%)				12	12

*All loads in lbs/ft; all dimensions in inches.

**Failure with local buckling at a perforation for sag rods.

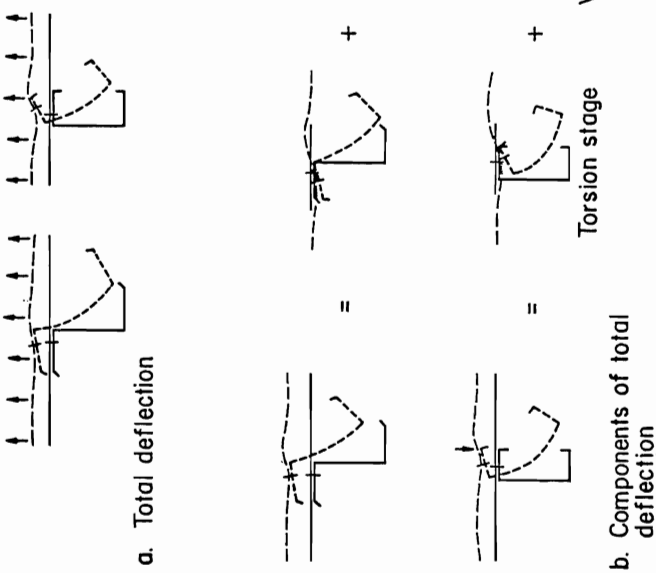

Fig. 1. Idealized Behavior of Purlins

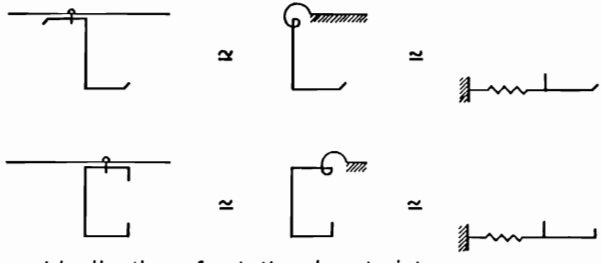

a. Idealization of rotational restraint

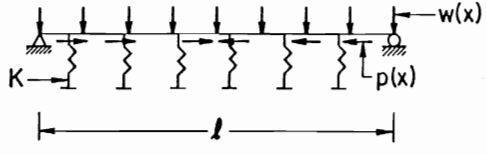

b. Beam-column idealization

Fig. 2. Behavior Idealization

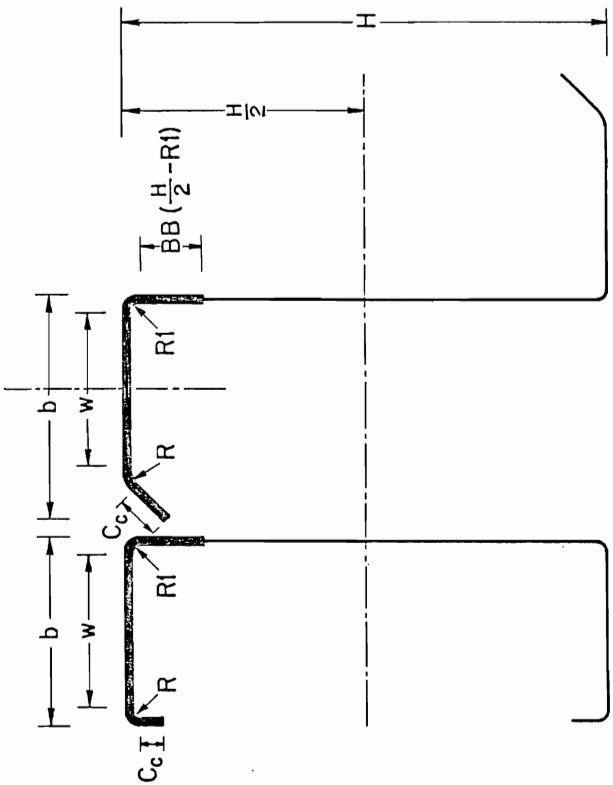

Fig. 3. Cross-Sectional Dimensions. The Heavy Lines Indicate the Idealized Beam-Column Section.

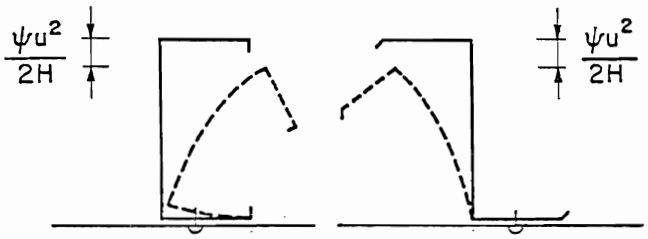

Fig. 4. Vertical Deflection Resulting from Lateral Deflection and Twist.

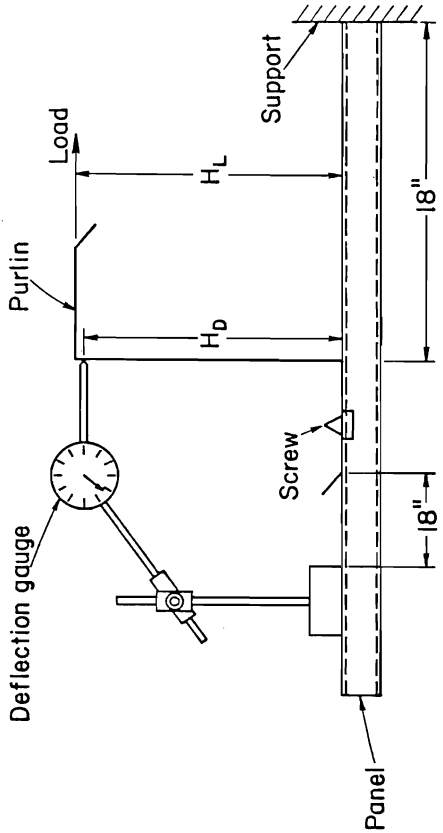

Fig. 5. F-Test: Diaphragm-Braced Purlin